ARTICLE NO. 79-0622R

J80-093

Transmission of Sound Through Nonuniform Circular Ducts with Compressible Mean Flows

20001

A. H. Nayfeh,* B. S. Shaker,† and J. E. Kaiser‡
Virginia Polytechnic Institute and State University, Blacksburg, Va.

An acoustic theory is developed to determine the sound transmission and attenuation through an infinite hard-walled or lined circular duct carrying compressible, sheared mean flows and having a variable cross section. The theory is applicable to large as well as small axial variations, as long as the mean flow does not separate. The technique is based on solving for the envelopes of the quasiparallel acoustic modes that exist in the duct instead of solving for the actual wave, thereby reducing the computation time and the round-off error encountered in purely numerical techniques. A number of test cases that demonstrate the flexibility of the program are included. Convergence of the transmission coefficients and the acoustic pressure profiles with in increasing number of modes is illustrated.

I. Introduction

THE trend toward the use of high-bypass turbojet engines has decreased jet noise and resulted in noise emissions from the inlet nacelles being responsible for an increasing proportion of community annoyance. Consequently, effective control measures are required to reduce the inlet noise to acceptable levels. The use of choked inlets has long been recognized as an effective means of reducing upstream noise propagation,[1,2] although such inlets require careful design to prevent excessive loss in compressor performance. Hence, a promising approach to the reduction of inlet noise is the use of a high-subsonic Mach number inlet, or partially choked inlet, in conjunction with an acoustic duct liner.

However, the physical mechanisms responsible for the noise reduction in high-subsonic Mach number inlets are not completely understood, and techniques for the theoretical analysis of sound propagation through regions of near-sonic mean flow are still in the development stage. Two major problems must be overcome in the development of such a model: 1) the mathematical techniques for the calculation of sound propagation in ducts are well developed for parallel ducts but are not fully developed for ducts of varying cross section that carry mean flows with strong axial and transverse gradients, and 2) linear acoustic equations are inadequate to describe acoustic propagation in regions of near-sonic mean flows. In the investigation reported herein, the first of these two problems was addressed, and a wave-envelope technique based on the method of variation of parameters was developed. This procedure can be used as the basis for the examination of the second aspect of the problem—the development of nonlinear models for the near-sonic region.

Several analytical as well as numerical techniques have been developed for the analysis of wave propagation in uniform and nonuniform ducts. Surveys of these techniques were made by Nayfeh et al.,[3] Nayfeh,[4] and Vaidya and Dean.[5] The approaches that have been developed for nonuniform ducts carrying a mean flow include quasi-one-dimensional approximations, multiple-scales solutions, solutions for weak wall undulations, weighted residual methods, as well as direct numerical integration. Each method has limitations either of a physical or computational nature. In the quasi-one-dimensional approach,[6-10] one examines only the lowest mode in ducts with slowly varying cross sections and thus cannot account for the effects of transverse mean-flow gradients or large wall admittance. Although the multiple-scales approach[11-13] permits the determination of the transmission and attenuation for all modes including the effects of transverse as well as axial gradients, the technique is limited to slow variations of the duct cross section and the expansion needs to be carried out to second order to determine reflections of the acoustic signal and intermodal coupling in transmission. In the weak-wall-undulation approach,[14] one obtains a perturbation solution for ducts whose walls deviate only slighly from the uniform case.

Finite-difference methods[15,16] have been applied to the case of uniform source inputs in nonuniform ducts. However, a large amount of computation will be required with these purely numerical techniques at high frequencies because a large number of grid points are needed to resolve the smallest wavelength. In addition, the determination of transmission and reflection characteristics of the duct modes would require the transverse step size to be small enough to resolve the highest mode. Thus, the computational time increases rapidly with increasing frequency and duct length, and the method is not well suited to the determination of transmission and reflection coefficients for large numbers of modes. To reduce the computational time for uniform-source and stepped-source inputs in a two-dimensional duct, Baumeister[17] used an estimate of the wavelength of the fundamental mode to explicitly express the fast axial variation and solved only for the envelope of the acoustic disturbance. The method of weighted residuals,[18] or Galerkin method, represents the acoustic signal as a linear superposition of basis functions, usually chosen to be the quasiparallel ducts modes, and thus is conveniently suited to the determination of transmission and reflection coefficients of the duct modes. However, the short axial wavelengths at high frequencies still require a large number of axial steps in the numerical computations.

In the work reported here, an acoustic theory was developed to determine the sound transmission and attenuation through an infinite, hard-walled or lined circular duct carrying compressible, sheared mean flows and having a variable cross section. In the development of the procedure, a

Presented as Paper 79-0622 at the AIAA 5th Aeroacoustics Conference, Seattle, Wash., March 12-14, 1979; submitted April 16, 1979; revision received Aug. 20, 1979.

Index category: Aeroacoustics.

*University Distinguished Professor, Dept. of Engineering Science and Mechanics. Member AIAA.

†Presently, Assistant Professor, King Abdulaziz University, Jeddah, Saudi Arabia.

‡Associate Professor, Dept. of Engineering Science and Mechanics. Member AIAA.

major goal was to achieve the capability of efficiently calculating transmission and reflection coefficients[19] of all interacting duct modes while retaining the ability to generate acoustic pressure and velocity distributions corresponding to specific acoustic inputs to the duct section. The technique employs features of several of the methods previously discussed. The computations of transmission and reflection coefficients for the duct are facilitated by representing the acoustic disturbance as a superposition of the quasiparallel duct modes. An explicit representation of the fast axial variation is included and only the slower variations of the mode amplitudes and phases are calculated. The method uses an integrability constraint that insures that it reduces to the multiple-scales solution as the duct variations become small. However, the theory is applicable to large as well as small axial variations as long as the mean flow does not separate. The feasibility of solving for the envelopes of the quasiparallel acoustic modes instead of solving for the actual wave has been demonstrated by Kaiser and Nayfeh[20] for plane ducts with no mean flow. A preliminary version of the wave-envelope procedure is described in Ref. 21.

Concurrently with the development of the wave-envelope method described herein, several finite-element methods[22-24] were developed for the study of transmission of sound in variable-area ducts with flow. The first method[22] employs a velocity-potential formulation of the basic equations; thus, it is restricted to irrotational mean flows. The others are more general in the sense that they permit the consideration of rotational mean flows. Eversman[23] compared transmission and reflection coefficients obtained from a finite-element procedure with those from the method of weighted residuals and found good agreement. Although the mean-flow model is rotational, it apparently does not include the refractive effect of a finite boundary-layer thickness at the duct walls. The finite-element method of Abrahamson[24] was developed for a general compressible mean flow, but it is currently implemented only for an incompressible model. Comparisons between results of this finite-element procedure and the wave-envelope method were carried out for cases of low-speed mean flows; an example of this comparison is included in Sec. V. These comparisons are of acoustic pressure distributions, since the finite-element program was not written to obtain transmission and reflection coefficients. Convergence of the results of the wave-envelope procedure with an increasing number of parallel-duct basis functions has been examined for cases both with and without mean flow.

II. Problem Formulation

The transmission and attenuation of sound in hard- and soft-walled circular ducts (Fig. 1) carrying viscous or inviscid compressible mean flows is examined. The mean Mach number in the throat is subsonic and the axial and radial gradients of the mean flow are not small. The cross section of the duct varies arbitrarily with the axial distance.

It is convenient to work with dimensionless quantities. To this end, velocities, lengths, and time are made dimensionless by using a convenient reference speed of sound c_a (taken to be the value at the duct entrance in the numerical studies), the radius R_0 of the duct in the uniform region (Fig. 1), and R_0/c_a, respectively. The pressure p is made dimensionless by using $\rho_a c_a^2$; the density ρ and temperature T are made dimensionless by using their corresponding reference values;

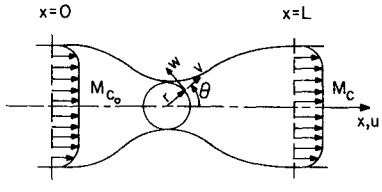

Fig. 1 Flow configuration.

and the viscosity μ and thermal conductivity κ are made dimensionless by using their wall values in the uniform section. In terms of these dimensionless variables, the equations which describe the unsteady viscous flow in a duct are (see, for example, Ref. 25):

Conservation of Mass:

$$\frac{\partial \rho}{\partial t} + \nabla \cdot (\rho v) = 0 \tag{1}$$

Conservation of Momentum:

$$\rho\left(\frac{\partial v}{\partial t} + v \cdot \nabla v\right) = -\nabla p + \frac{1}{Re}\nabla \cdot \tau \tag{2}$$

Conservation of Energy:

$$\rho\left(\frac{\partial T}{\partial t} + v \cdot \nabla T\right) - (\gamma - 1)\left(\frac{\partial p}{\partial t} + v \cdot \nabla p\right) = \frac{1}{Re}\left[\frac{1}{Pr}\nabla \cdot (\kappa \nabla T) + (\gamma - 1)\Phi\right] \tag{3}$$

Equation of State: For a perfect gas,

$$\gamma p = \rho T \tag{4}$$

where v is the velocity vector, t is the time, γ is the ratio of the gas specific heats, $Pr = \mu_w C_p/\kappa_w$ is the Prandtl number, C_p is the gas specific heat at constant pressure, and $Re = \rho_a c_a R_0/\mu_w$ is the Reynolds number. The subscript w refers to conditions at the duct wall.

In general, the ducts carry a high-subsonic, steady, sheared mean flow that satisfies Eqs. (1-4). The presence of sound in the ducts results in the perturbation of the flow quantities so that

$$q(r,t) = q_0(r) + q_1(r,t) \tag{5}$$

where q stands for any flow quantity, r is the position vector, q_0 is the mean flow, and q_1 is the acoustic part. The usual simplifying assumptions of negligible nonlinear and viscous terms in the acoustic equations are made. The assumption of linearization is not valid for high sound-pressure levels, and, in particular, the nonlinearity of the gas must be included when the mean flow is near sonic (i.e., near the throat). Further, the decrease in axial wavelength of the upstream propagating acoustic signal as it approaches a near-sonic region and the nonlinear transfer of energy to higher harmonics can cause some viscous terms to become significant. The relative importance of the nonlinear and viscous terms is now under investigation, but for the investigation reported here, the Mach number at the throat is restricted to values not too close to unity so that the linear, inviscid model is adequate. In addition, mean flows with swirl are excluded from this study so that mean-flow quantities are a function only of the radial and axial coordinates.

A cylindrical coordinate system (r,θ,x) is introduced, as shown in Fig. 1. Since there is no swirling flow, each acoustic quantity $q_1(r,x,\theta,t)$ can be expressed for sinusoidal time variation as

$$q_1(r,x,\theta,t) = \sum_{m=0}^{\infty} q_{1_m}(r,x)\exp[-i(\omega t + m\theta)] \tag{6}$$

where ω is the dimensionless frequency. Using the preceding assumptions, one can rewrite the governing equations in

cylindrical coordinates as

$$-i\omega\rho_1+\frac{\partial}{\partial x}(\rho_0u_1+u_0\rho_1)+\frac{i\rho_0m}{r}w_1$$

$$+\frac{1}{r}\frac{\partial}{\partial r}(r\rho_0v_1+rv_0\rho_1)=0 \tag{7}$$

$$\rho_0\left[-i\omega u_1+\frac{\partial}{\partial x}(u_0u_1)+v_0\frac{\partial u_1}{\partial r}+v_1\frac{\partial u_0}{\partial r}\right]$$

$$+\rho_1\left[u_0\frac{\partial u_0}{\partial x}+v_0\frac{\partial u_0}{\partial r}\right]=-\frac{\partial p_1}{\partial x} \tag{8}$$

$$\rho_0\left[-i\omega v_1+\frac{\partial}{\partial r}(v_0v_1)+u_0\frac{\partial v_1}{\partial x}+u_1\frac{\partial v_0}{\partial x}\right]$$

$$+\rho_1\left[v_0\frac{\partial v_0}{\partial r}+u_0\frac{\partial v_0}{\partial x}\right]=-\frac{\partial p_1}{\partial r} \tag{9}$$

$$\rho_0\left[-i\omega w_1+v_0\frac{\partial w_1}{\partial r}+\frac{v_0w_1}{r}+u_0\frac{\partial w_1}{\partial x}\right]=-\frac{im}{r}p_1 \tag{10}$$

$$\rho_0\left[-i\omega T_1+v_0\frac{\partial T_1}{\partial r}+u_0\frac{\partial T_1}{\partial x}+v_1\frac{\partial T_0}{\partial r}\right.$$

$$\left.+u_1\frac{\partial T_0}{\partial x}\right]+\rho_1\left[v_0\frac{\partial T_0}{\partial r}+u_0\frac{\partial T_0}{\partial x}\right]$$

$$-(\gamma-1)\left[-i\omega p_1+u_0\frac{\partial p_1}{\partial x}+v_0\frac{\partial p_1}{\partial r}\right.$$

$$\left.+u_1\frac{\partial p_0}{\partial x}+v_1\frac{\partial p_0}{\partial r}\right]=0 \tag{11}$$

$$\frac{p_1}{p_0}=\frac{\rho_0}{\rho_0}+\frac{T_1}{T_0} \tag{12}$$

where u, v, and w are the velocities in the axial, radial, and azimuthal directions, respectively, and the subscript m has been suppressed.

To complete the problem formulation, one needs to specify the initial and boundary conditions. The boundary conditions are based on the assumption that the duct wall is lined with a point-reacting acoustic material whose specific acoustic admittance β may vary along the duct. For no-slip mean flows, a requirement of continuity of the particle displacement gives

$$v_1-R'u_1=(\beta/\rho_wc_w)p_1\sqrt{1+R'^2}\ \text{ at } r=R \tag{13}$$

where R' is the slope of the wall and the subscript w refers to values at the wall. Since the results are desired in the form of transmission and reflection matrices for a given duct section, the initial conditions consist of the successive input of each acoustic mode at the duct entrance.

III. Form of Solution

The method of variation of parameters is used to change the dependent variables from fast-varying variables to others that vary slowly. Moreover, the solution is approximated by a finite sum of the quasiparallel duct eigenfunctions.

Thus, we seek an approximate solution to Eqs. (7-13) in the form

$$p_1\simeq\sum_{n=1}^{N}\left\{A_n(x)\psi_n^p(r,x)\exp\left(i\int k_n(x)\,dx\right)\right.$$

$$\left.+\tilde{A}_n(x)\tilde{\psi}_n^p(r,x)\exp\left(i\int\tilde{k}_n(x)\,dx\right)\right\} \tag{14}$$

$$u_1\simeq\sum_{n=1}^{N}\left\{A_n(x)\psi_n^u(r,x)\exp\left(i\int k_n(x)\,dx\right)\right.$$

$$\left.+\tilde{A}_n(x)\tilde{\psi}_n^u(r,x)\exp\left(i\int\tilde{k}_n(x)\,dx\right)\right\} \tag{15}$$

with similar expressions for v_1, w_1, T_1, and ρ_1, where the tilde refers to upstream propagation, the $\psi_n(r,x)$ are the quasiparallel mode shapes corresponding to the quasiparallel propagation coefficients $k_n(x)$, and the $A_n(x)$ are complex functions whose moduli and arguments represent, in some sense, the amplitudes and phases of the (m,n) modes. The circumferential model number m is assumed to be specified and the corresponding subscript on A, ψ, and k is not explicitly stated; each variable is expressed as a summation over a finite number of radial modes n, with $n=1$ denoting the fundamental radial mode rather than the conventional $n=0$. Since k_n is complex, the exponential factor contains an estimate of the attenuation of the (m,n) mode, as well as the axial oscillations of the acoustic modes.

Since the ψ_n are the quasiparallel mode shapes, they are the solutions of the following problem:

$$-i\hat{\omega}\psi^p+ik\rho_0\psi^u+\frac{i\rho_0m}{r}\psi^w+\frac{1}{r}\frac{\partial}{\partial r}(r\rho_0\psi^v)=0 \tag{16}$$

$$-i\rho_0\hat{\omega}\psi^u+\rho_0\frac{\partial u_0}{\partial r}\psi^v+ik\psi^p=0 \tag{17}$$

$$-i\rho_0\hat{\omega}\psi^v+\frac{\partial\psi^p}{\partial r}=0 \tag{18}$$

$$-i\rho_0\hat{\omega}\psi^w+\frac{im}{r}\psi^p=0 \tag{19}$$

$$-i\rho_0\hat{\omega}\psi^T+\rho_0\frac{\partial T_0}{\partial r}\psi^v+i(\gamma-1)\hat{\omega}\psi^p=0 \tag{20}$$

$$\frac{\psi^p}{p_0}=\frac{\psi^\rho}{\rho_0}+\frac{\psi^T}{T_0} \tag{21}$$

$$\psi^v-\frac{\beta}{\rho_wc_w}\psi^p=0\ \text{ at } r=R \tag{22}$$

where

$$\hat{\omega}=\omega-ku_0 \tag{23}$$

Equations (16-23) can be combined to yield the well-known problem for parallel-duct eigenfunctions:

$$\frac{\partial^2\psi^p}{\partial r^2}+\left[\frac{1}{r}+\frac{T_0'}{T_0}+\frac{2ku_0'}{\hat{\omega}}\right]\frac{\partial\psi^p}{\partial r}+\left[\frac{\hat{\omega}^2}{T_0}-k^2-\frac{m^2}{r^2}\right]\psi^p=0 \tag{24}$$

$$\frac{\partial\psi^p}{\partial r}-i\frac{\omega\beta}{T_w^{1/2}}\psi^p=0\ \text{ at } r=R \tag{25}$$

At each axial location, the solution of Eqs. (24) and (25) yields $\psi_n^p(r;x)$ and its corresponding propagation coefficient $k_n(x)$. Since the basis functions $\psi_n^p(r;x)$ vary in the axial direction, they must be normalized in some manner to provide significance to the axial variations of the mode amplitudes. The normalization used in this study is the same as that defined by Zorumski[19]:

$$\int_0^R r[\psi_n^p(r;x)]^2\,dr=1 \tag{26}$$

Then, Eqs. (16-21) are used to express the mode shapes of the other flow variables in terms of ψ_n^p and k_n.

Since the transverse dependence in the assumed solution, Eqs. (14) and (15), is chosen a priori, it cannot satisfy Eqs. (7-12) exactly. Thus, the assumed solution must be subjected to constraints. Rather than using the usual method of weighted residuals which forces the residuals in each of the basic Eqs. (7-12) and the boundary condition, Eq. (13), to be orthogonal to some a priori chosen functions, we require the deviations from the quasiparallel solution to be orthogonal to every solution of the adjoint quasiparallel problem. This approach assures the recovery of the results of method of multiple scales[26] when the axial variations are slow.[20] In addition, it leads to a set of ordinary differential equations whose number is smaller and whose coefficient matrix is better conditioned than for those equations obtained with the usual weighted-residual approach.

To enforce the constraints, one must define the problem adjoint to the quasiparallel problem. To this end,[27] one can multiply Eqs. (16-21) by the functions $\phi_1,\phi_2,\phi_3,\phi_4,\phi_5$, and ϕ_6, respectively, where the $\phi_n(r,x)$ are solutions of the adjoint problem, add the resulting equations, integrate the result by parts from $r=0$ to $r=R$, thereby transferring the r derivatives from the ψ's to the ϕ's, and obtain

$$\int_0^R \psi^p[-i\hat{\omega}\phi_1-\phi_6/\rho_0]\mathrm{d}r+\int_0^R i\rho_0\psi^u[-\hat{\omega}\phi_2 +k\phi_1]\mathrm{d}r+\int_0^R \rho_0\psi^v\left[-i\hat{\omega}\phi_3+\frac{\partial u_0}{\partial r}\phi_2 -r\frac{\partial}{\partial r}\left(\frac{\phi_1}{r}\right)+\frac{\partial T_0}{\partial r}\phi_5\right]\mathrm{d}r +\int_0^R i\rho_0\psi^w\left[-\hat{\omega}\phi_4+\frac{m}{r}\phi_1\right]\mathrm{d}r+\int_0^R \psi^p[ik\phi_2 -\frac{\partial\phi_3}{\partial r}+\frac{im}{r}\phi_4+i(\gamma-1)\hat{\omega}\phi_5+\phi_6/p_0]\mathrm{d}r +\int_0^R \rho_0\psi^T[-i\hat{\omega}\phi_5-p_0\phi_6]\mathrm{d}r+[\rho_0\psi^v\phi_1+\psi^p\phi_3]_0^R=0 \quad (27)$$

Then, the adjoint equations are obtained by setting each of the brackets in the integrands of Eq. (27) to zero; for example,

$$i\hat{\omega}\phi_1+\phi_6/\rho_0=0, \text{ etc.} \quad (28)$$

From these adjoint equations, one can express each of the ϕ_n as a function of ϕ_1:

$$\phi_2=(k/\hat{\omega})\phi_1 \quad (29)$$

$$\phi_3=\frac{irT_0}{\hat{\omega}^2}\frac{\partial}{\partial r}\left(\frac{\hat{\omega}\phi_1}{rT_0}\right) \quad (30)$$

$$\phi_4=m\phi_1/r\hat{\omega} \quad (31)$$

$$\phi_5=\phi_1/T_0 \quad (32)$$

$$\phi_6=-i\rho_0\hat{\omega}\phi_1 \quad (33)$$

Using Eqs. (29-33) in the remaining adjoint equation, one then obtains the governing equation for ϕ_1:

$$\frac{1}{r}\frac{\partial}{\partial r}\left[\frac{rT_0}{\hat{\omega}^2}\frac{\partial\eta}{\partial r}\right]+\left[1-\frac{T_0k^2}{\hat{\omega}^2}-\frac{T_0m^2}{r^2\hat{\omega}^2}\right]\eta=0 \quad (34)$$

where

$$\eta=\phi_1\hat{\omega}/rT_0 \quad (35)$$

It can be shown easily that Eqs. (24) and (34) are the same; thus η and ψ^p satisfy the same differential equation. Further, after the adjoint equations are removed from Eq. (27), the remaining boundary terms can be simplified using Eqs. (18, 30, and 35) to obtain

$$\frac{\partial\eta}{\partial r}-\frac{i\omega\beta}{T_w^{1/2}}\eta=0 \text{ at } r=R \quad (36)$$

Since the boundary condition, Eq. (36), is the same as the boundary condition, Eq. (25), one concludes that $\eta=\psi^p$ without loss of generality. Thus, one needs only to solve the quasiparallel problem to determine ψ_n^p and then determine ϕ_{1_n} from

$$\phi_{1_n}=rT_0\psi_n^p/\hat{\omega} \quad (37)$$

The remaining ϕ's are then determined from Eqs. (29-33).

Once the adjoint functions are known, the constraint conditions are determined as follows. On multuplying Eqs. (7-12) by ϕ_{1_n}, $\phi_{2_n},\ldots,\phi_{6_n}$, respectively, adding the resulting equations, integrating the result by parts from $r=0$ to $r=R$ to transfer the r derivatives to the ϕ's, and using the adjoint equations and Eq. (13), one obtains the following constraint:

$$\int_0^R\Big\{\phi_{1_n}[-iu_0k_n\rho_1-ik_n\rho_0u_1+\frac{\partial}{\partial x}(\rho_0u^1+u_0\rho_1)] -rv_0\rho_1\frac{\partial}{\partial r}\left(\frac{\phi_{1n}}{r}\right)+\phi_{2_n}\Big[-iu_0k_n\rho_0u_i-ik_np_1+\rho_0\frac{\partial(u_0u_1)}{\partial x} +\rho_1\left(u_0\frac{\partial u_0}{\partial x}+v_0\frac{\partial u_0}{\partial r}\right)+\frac{\partial p_1}{\partial x}\Big]-u_1\frac{\partial}{\partial r}(\rho_0v_0\phi_{2_n}) +\phi_{3_n}\Big[-iu_0k_n\rho_0v_1+\rho_0u_0\frac{\partial v_1}{\partial x}+\rho_0u_1\frac{\partial v_0}{\partial x} +\rho_1\left(v_0\frac{\partial v_0}{\partial r}+u_0\frac{\partial v_0}{\partial x}\right)\Big]-v_0v_1\frac{\partial}{\partial r}(\rho_0\phi_{3_n}) +\phi_{4_n}\Big[-ik_n\rho_0u_0w_1+\frac{\rho_0v_0w_1}{r}+\rho_0u_0\frac{\partial w_1}{\partial x}\Big] -w_1\frac{\partial}{\partial r}(\rho_0v_0\phi_{4_n})+\phi_{5_n}\Big[-iu_0k_n\rho_0T_1+(\gamma-1)iu_0k_np_1 +\rho_0u_0\frac{\partial T_1}{\partial x}+\rho_0u_0\frac{\partial T_0}{\partial x}+\rho_1\left(v_0\frac{\partial T_0}{\partial r}+u_0\frac{\partial T_0}{\partial x}\right) -(\gamma-1)\left(u_0\frac{\partial p_1}{\partial x}+u_1\frac{\partial p_0}{\partial x}+v_1\frac{\partial p_0}{\partial r}\right)\Big] -T_1\frac{\partial}{\partial r}(\rho_0v_0\phi_{5_n})+(\gamma-1)p_1\frac{\partial}{\partial r}(v_0\phi_{5_n})\Big\}\mathrm{d}r +\rho_0\phi_1\Big[R'u_1+\frac{\beta}{\rho_wc_w}p_1(\sqrt{1+R'^2}-1)\Big]_{r=R}=0 \quad (38)$$

Substitution of the assumed solution, Eqs. (14) and (15), into Eq. (38) yields the following $2N$ equations for the A's:

$$\sum_{n=1}^{2N} f_{mn}\frac{\mathrm{d}A_n}{\mathrm{d}x}=\sum_{n=1}^{2N} g_{mn}A_n \quad (39)$$

where $m=1, 2, 3,\ldots, 2N$ and

$$f_{mn}=\Big[\int_0^R\{\phi_{1_m}(\rho_0\psi_n^u+u_0\psi_n)+\phi_{2_m}(\rho_0u_0\psi_n^u+\psi_n^p)$$

$$+\phi_{3_m}(\rho_0 u_0 \psi_n^v + \phi_{4_m}\rho_0 u_0 \psi_n^w + \phi_{5_m}((\rho_0 u_0 \psi_n^T - (\gamma-1)u_0\psi_n^p)\}\mathrm{d}r\Big]e^{i\int k_n \mathrm{d}x} \quad (40)$$

$$g_{mn} = -\Big[\int_0^R \Big\{\phi_{1_m}\Big[\frac{\partial}{\partial x}(\rho_0\psi_n^u + u_0\psi_n^\rho)\Big] - rv_0\psi_n^\rho\frac{\partial}{\partial r}\Big(\frac{\phi_{1m}}{r}\Big)$$

$$+\phi_{2_m}\Big[\rho_0\frac{\partial}{\partial x}(u_0\psi_n^u) + \psi_n^\rho\Big(u_0\frac{\partial u_0}{\partial x} + v_0\frac{\partial u_0}{\partial r}\Big) + \frac{\partial\psi_n^p}{\partial x}\Big]$$

$$-\psi_n^u\frac{\partial}{\partial r}(\rho_0 v_0\phi_{2_m}) + \phi_{3_m}\Big[\rho_0 u_0\frac{\partial\psi_n^v}{\partial x} + \rho_0\psi_n^u\frac{\partial v_0}{\partial x} + \psi_n^\rho\Big(v_0\frac{\partial v_0}{\partial r}$$

$$+u_0\frac{\partial v_0}{\partial x}\Big)\Big] - v_0\psi_n^v\frac{\partial}{\partial r}(\rho_0\phi_{3_m}) + \phi_{4_m}\Big[\frac{\rho_0 v_0\psi_n^w}{r} + \rho_0 u_0\frac{\partial\psi_n^w}{\partial x}\Big]$$

$$-\psi_n^w\frac{\partial}{\partial r}(\rho_0 v_0\phi_{4_m}) + \phi_{5_m}\Big[\rho_0 u_0\frac{\partial\psi_n^T}{\partial x} + \rho_0\psi_n^u\frac{\partial T_0}{\partial x}$$

$$+\psi_n^\rho\Big(v_0\frac{\partial T_0}{\partial r} + u_0\frac{\partial T_0}{\partial x}\Big) - (\gamma-1)\Big(u_0\frac{\partial\psi_n^p}{\partial x} + \psi_n^u\frac{\partial p_0}{\partial x}$$

$$+\psi_n^v\frac{\partial p_0}{\partial r}\Big)\Big] - \psi_n^T\frac{\partial}{\partial r}(\rho_0 v_0\phi_{5_m}) + (\gamma-1)\psi_n^p\frac{\partial}{\partial r}(v_0\phi_{5_m}) + \phi_{1_m}$$

$$\times i(k_n-k_m)(\rho_0\psi_n^u + u_0\psi_n^\rho) + \phi_{2_m}i(k_n-k_m)(\psi_n^p + \rho_0 u_0\psi_n^u)$$

$$+\phi_{3_m}i(k_n-k_m)\rho_0 u_0\psi_n^v\phi_{4_m}i(k_n-k_m)\rho_0 u_0\psi_n^w$$

$$+\phi_{5_m}i(k_n-k_m)u_0\times(\rho_0\psi_n^T - (\gamma-1)\psi_n^p)\Big\}\mathrm{d}r$$

$$+\rho_0\phi_{1_m}\Big[R'\psi_n^u + \frac{\beta}{\rho_w c_w}\psi_n^p(\sqrt{1+R'^2}-1)\Big]_{r=R}\Big]e^{i\int k_n\mathrm{d}x} \quad (41)$$

For convenience, the upstream modes are now denoted by A_n, $n=N+1,\ldots,2N$, i.e.,

$$A_{N+n} = \tilde{A}_n \quad n=1,2,3,\ldots N$$

IV. Numerical Solution

To evaluate the coefficients f_{mn} and g_{mn} of the set of ordinary-differential equations for the mode amplitudes A_n, one must specify all mean-flow variables, u_0,ρ_0,T_0,p_0,v_0, and their first partial derivatives with respect to both x and r. The form of g_{mn} as given in Eq. (41) would also require some second derivatives. However, those terms involving second derivatives have been integrated by parts and the resulting expression for g, which requires only first derivatives of the mean flow, has been used in the numerical development. Any suitable method of solution for the mean flow can be used in conjunction with the acoustic program, provided it is capable of supplying the variables and their first derivatives and provided it supplied velocity fields that satisfy the no-slip boundary condition at the wall.

For the present study, a simplified model of the mean flow has been employed. This model uses a one-dimensional gasdynamics theory to describe the mean-flow variables in the inviscid core; thus, u_0,p_0,T_0, and ρ_0 are constant across the duct cross section, except in the region of the wall boundary layer. The program permits one to select one of two options: the radial velocity v_0 can be set equal to zero, consistent with the one-dimensional theory, or the radial velocity can be calculated to be a linear function of r, consistent with the mean-continuity equation and the flow-tangency condition at the wall. Several velocity profiles in the wall boundary layer have been examined; most of the results have been obtained using a quarter-sine profile; that is,

$$\frac{u_0}{u_c} = \sin[\pi(R-r)/2\delta] \quad \text{for } r \geq R-\delta = 1$$
$$\text{for } r \leq R-\delta \quad (42)$$

The temperature profile is related to the velocity profile by[25]

$$\frac{T_0}{T_c} = 1 + r_1\frac{\gamma-1}{2}M_c^2\Big[1-\Big(\frac{u_0}{u_c}\Big)^2\Big] + \frac{T_w - T_{ad}}{T_c}\Big[1-\frac{u_0}{u_c}\Big] \quad (43a)$$

$$\frac{T_{ad}}{T_c} = 1 + r_1\frac{\gamma-1}{2}M_c^2 \quad (43b)$$

where the subscript c refers to values in the inviscid core, T_w is the wall temperature, T_{ad} is the adiabatic wall temperature, δ is the boundary-layer thickness, r_1 is the recovery factor, and $\gamma = 1.4$ is the ratio of the gas specific heats. For variable-area ducts, the use of Eqs. (43) can be considered a rough approximation only, providing the user with a means of checking the sensitivity of the results to changes in the mean temperature profile. To this end, three options have been provided for selection of the wall temperature: the wall temperature can be set to any specified constant value, it can be set equal to the inviscid core value T_c, or it can be set equal to the adiabatic wall temperature T_{ad}.

The axial variation of the boundary-layer displacement thickness δ_1 is assumed to be known and is specified in the program by a simple polynomial variation. Specification of the mean-flow Mach number at $x=0$ permits the subsequent axial variations of δ and M_c to be calculated from the definition of displacement thickness and from mass flow considerations. The one-dimensional gasdynamics theory provides the axial variation of T_c,ρ_c,u_c, etc., and the boundary-layer profiles are computed from Eqs. (42) and (43).

The wall of the duct is assumed to be lined; the admittance of the liner is taken to vary from a specified value β_0 at $x=0$ to a specified value β_L at $x=L$ according to the expression

$$\beta = \beta_0 + (\beta_L - \beta_0)(3-2x/L)(x/L)^2 \quad (44)$$

This gives a continuously varying admittance with $\mathrm{d}\beta/\mathrm{d}x = 0$ at both $x=0$ and $x=L$.

The quasiparallel acoustic Eqs. (24) and (25) are solved at each axial position by using a fourth-order Runge-Kutta technique and by employing a Newton-Raphson procedure to determine the eigenvalues k_n. The accuracy of the Runge-Kutta procedure should assure good numerical results with a minimum of grid points across the duct width.

To determine the coefficients g_{mn} of Eq. (41), one has to evaluate the axial gradients of the wavenumber k and of the eigenfunctions ψ_n. These axial derivatives are obtained by using a simple finite-difference quotient.

The adjoint functions are found from the quasiparallel variables ψ^p, $\partial\psi^p/\partial x$, and k by using the relations, Eqs. (29-35). The coefficients f_{mn} and g_{mn} are then evaluated from Eqs. (40) and (41). The integrals across the duct in these expressions are evaluated using Simpson's rule which yields a high level of accuracy. The axial integrals $\int k_n \mathrm{d}x$ are evaluated with the trapezoid rule, which is of sufficient accuracy to obtain good convergence with changes in Δx.

Writing Eq. (39) in matrix form, $F\mathrm{d}A/\mathrm{d}x = GA$, and solving for $\mathrm{d}A/\mathrm{d}x$, one obtains

$$\mathrm{d}A/\mathrm{d}x = F^{-1}GA \quad (45)$$

where A is a column vector whose elements are A_n. A Runge-Kutta forward-integation technique is used to solve Eq. (45) for the function A at each axial station. Since the problem is linear, one can determine the solution for any problem subject to general boundary conditions at the two ends of the duct by a linear combination of $2N$ linearly independent solutions.

The linearly independent solutions are obtained by setting all mode amplitudes except one equal to zero at $x=0$ and integrating Eq. (45) to $x=L$. One such integration for each of the $2N$ modes allows one to obtain the transfer matrices TR_1, TR_2, TR_3, and TR_4 which are defined by

$$B^+(L) = TR_1 B^+(0) + TR_2 B^-(0) \tag{46a}$$

$$B^-(L) = TR_3 B^+(0) + TR_4 B^-(0) \tag{46b}$$

where $B^+(x)$ is a column vector of the amplitudes $A_n e^{i\int k_n dx}$ of the right-running modes and $B^-(x)$ is a column vector of the amplitudes $\bar{A}_n e^{i\int k_n dx}$ of the left-running modes. Thus, the transfer matrices allow one to calculate the complex-mode amplitudes at $x=L$ from those at $x=0$. Following Ref. 19, we derive results in the form of transmission and reflection coefficients for the variable-area segment being considered. The transmission and reflection coefficients for the variable-area segment being considered. The transmission and reflection coefficients relate the complex magnitudes of the outgoing modes to those of the incoming modes,

$$B^+(L) = T^{L,0} B^+(0) + R^{L,L} B^-(L) \tag{47a}$$

$$B^-(0) = T^{0,L} B^-(L) + R^{0,0} B^+(0) \tag{47b}$$

and are calculated from the transfer matrices by[20]:

$$\begin{aligned} T^{0,L} &= TR_4^{-1} \\ R^{0,0} &= -TR_4^{-1} TR_3 \\ R^{L,L} &= TR_2 TR_4^{-1} \\ T^{L,0} &= TR_1 + TR_2 R^{0,0} \end{aligned} \tag{48}$$

The (m,n) term of $T^{L,0}$ represents the transmission of the mth radial mode at $x=L$ due to the nth radial mode being incident at $x=0$, etc. The requirement that the procedure be able to calculate these transmission and reflection coefficients makes a direct numerical procedure undesirable for this study. The wave-envelope, eigenfunction-expansion procedure developed in Sec. III is better suited to the necessary repetitive calculations with each mode as input than a direct numerical approach would be. Futher, it is noted that the transmission and reflection coefficients are general—no assumption about the nature of the source input to the duct has been made.

In addition to the calculation of the transmission and reflection coefficients, the acoustic pressure distributions can be constructed if the input to the duct section is specified. Specifically, one must designate the values of $B^+(0)$ and $B^-(L)$, which are the amplitudes of the right-running modes that are incident on the duct section at $x=0$ and the amplitudes of the left-running modes that are incident on the duct section at $x=L$, respectively. The program stores the values necessary to construct the pressure distribution across the duct:

$$p_l(r,x,\theta,t) = \left[\sum_{n=1}^{N} B_n^+(x) \psi_n^p(r,x) + \sum_{n=1}^{N} B_n^-(x) \tilde{\psi}_n^p(r,x) \right] e^{i(m\theta - \omega t)} \tag{49}$$

where the bracketed terms describe the spatial distribution of interest. A similar expression is evaluated for the acoustic particle velocity (axial component) and the moduli and arguments of these quantities are output of the program.

The accuracy of these acoustic-pressure and velocity profiles depends on the accuracy of the eigenfunction expansion procedure that forms the basis of this study. General guidelines are available from parallel duct studies (for example, Hersh and Catton[28] and Unruh and Eversman[29]); eigenvalues and attenuation rates (transmission and reflection coefficients in the variable-area case) converge more rapidly with an increasing number of basis functions than does the eigenfunctions (pressure profiles in the variable-area case). By using the parallel-duct eigenfunctions as the basis functions, one should minimize any convergence problems if all cut-on modes are included in the analysis; the magnitudes of any cut-off modes should be sufficiently small so as not to cause a large error. In addition, the integrability constraint developed in Sec. III assures that the governing equations are satisfied "on the average" at each cross section; that is, the average error at any cross section will be zero even if an inadequate number of modes is used. Thus, the overall characteristics of the duct, such as transmission and reflection coefficients, are more accurate than the details of the acoustic pressure distributions.

V. Results

Testing the method of solution is somewhat difficult since there are few available solutions for acoustic propagation through variable-area ducts carrying a high-speed, compressible mean flow, other than one-dimensional solutions. However, a few tests can be conducted for simple flows to determine the internal consistency of the program.

For straight, uniform ducts, the wave-envelope amplitudes are correctly calculated to be constant throughout the duct, and the routine for solving the parallel-duct eigenfunctions and eigenvalues produces the expected results. In addition, a number of symmetry checks on the transmission and reflection coefficients can be performed for both straight and variable-area ducts with and without either liners or mean flows. For example, in straight-lined ducts without flow, the reflection coefficients should be identically zero, and the off-diagonal terms of the transmission matrices should be zero; further, $T^{L,0}$ should be equal to $T^{0,L}$ because the left-running and right-running modes are identical. For variable-area, lined ducts without flow, reflection and intermodal coupling in the transmission coefficients is expected to be nonzero; however, the symmetry of the situation still requires $T^{0,L}=T^{L,0}$ and $R^{0,0}=R^{L,L}$. These expected results are achieved to a high degree of accuracy in a number of test cases that have been calculated. For variable-area, lined ducts that carry a mean flow, the transmission coefficients $T^{L,0}$ for a case when $M>0$ (mean flow from left to right) should be the same as the coefficients $T^{0,L}$ for a case when $M<0$ (mean flow from right to left) provided all duct properties and the mean flow are symmetric about $x=L/2$. Similar arguments can be made for the reflection coefficients. For a dimensionless frequency $\omega=10$ and an axisymmetric acoustic disturbance $m=0$, one example of such results yields for $M_{c_0}=+0.3$,

$$T^{L,0} = \begin{bmatrix} 0.51771+0.29426i & 0.37739-0.27368i \\ 0.38645-0.31743i & -0.06760+0.36536i \end{bmatrix}$$

and for $M_{c_0}=-0.3$,

$$T^{0,L} = \begin{bmatrix} 0.51790+0.29418i & 0.37744-0.27382i \\ 0.38650-0.31753i & -0.06748+0.36548i \end{bmatrix}$$

The agreement between $T^{0,L}$ for $M_0=+0.3$ for $M_0=-0.3$ is comparable to that just shown, and the agreement for reflection coefficients is better. Since the largest errors are in the fourth decimal place, the results are considered to be satisfactory. In these variable-area cases, the duct radius is assumed to have a simple converging-diverging variation with axial distance:

$$R = 1 + a_2(-1+\cos 2\pi x/L)$$

Table 1 Convergence of transmission coefficients

N	$T^{L,0}_{11}$	$T^{L,0}_{12}$	$T^{L,0}_{13}$	$T^{L,0}_{14}$	$T^{L,0}_{15}$	$T^{L,0}_{16}$
1	$-0.323-0.907i$					
2	$-0.251-0.828i$	$-0.291-0.349i$				
3	$-0.238-0.825i$	$-0.309-0.350i$	$0.080+0.017i$			
4	$-0.236-0.826i$	$-0.311-0.348i$	$0.081+0.012i$	$-0.012+0.011i$		
5	$-0.236-0.827i$	$-0.311-0.348i$	$0.081+0.012i$	$-0.011+0.011i$	$0.001-0.003i$	
6	$-0.236-0.827i$	$-0.311-0.348i$	$0.081+0.012i$	$-0.011+0.011i$	$0.001-0.003i$	$0.0005+0.0001i$

In the preceding case, the mean-flow Mach number reaches a value of 0.61 at the throat; this value is sufficiently large for compressibility effects to be important.

An example that demonstrates the computational advantage of the wave-envelope method is illustrated in Fig. 2. In this figure, the development of the (2,0) mode (second spinning mode, fundamental radial mode) in the converging portion of a lined duct is shown; the mean-flow Mach number varies from 0.1 at $x=0$ to 0.162 at $x=1$ and the boundary-layer thickness grows slightly in this region. The axial wavelength at this frequency, $\omega=7$, is roughly the same as the length of the converging portion of the duct; at higher frequencies, the variation would be more rapid with axial distance. However, the computational procedure requires a numerical integration only to generate the function A_j; the slow variation of this function requires fewer numerical steps than would a direct integration through each axial wavelength of the acoustic disturbance. It is noted that the function A_j is not the actual wave envelope of the acoustic disturbance; rather, the deviation of the function A_j from unity is an indication of how much the solution deviates from a parallel-duct eigenfunction solution. The axial variation of the parameter A_j, shown in Fig. 2, is representative of the variations calculated in most cases; however, there are some instances in which the parameters A_n may undergo fairly large variations if the parallel-duct solution is a poor approximation in some region of the duct. Overall, however, the wave-envelope procedure has been found to be numerically superior.

It is anticipated that the results will be accurate if all cut-on modes are included in the calculation. As a test, two cases for $\omega=18$ are considered in which there are six cut-on modes in each direction. Calculations are made with fewer modes in order to check the convergence of the results as the number of modes is increased. The first case discussed here is a straight duct with no mean flow and lined with a variable-admittance liner. Figure 3 shows the various approximations of the pressure profile midway through the duct for the case when the lowest mode is input at $x=0$. It is seen that the convergence is slowest at the duct centerline, fastest at the wall,

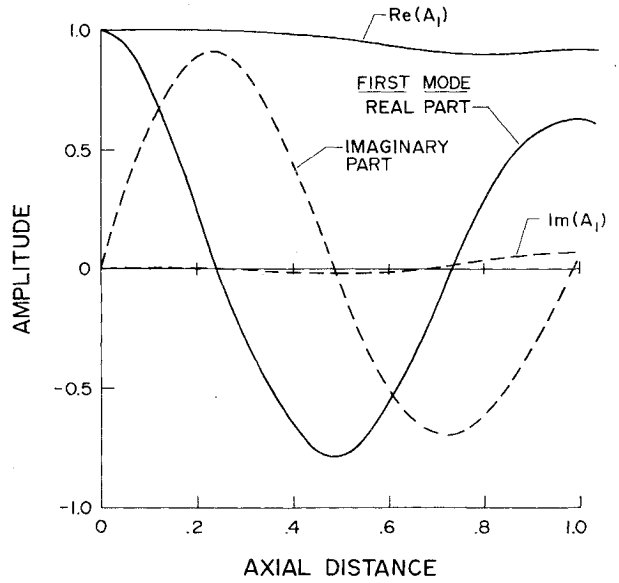

Fig. 2 Comparison between the fast varying function $A_j\exp(\int ik_j\,dx)$ and the slowly varying function A_j.

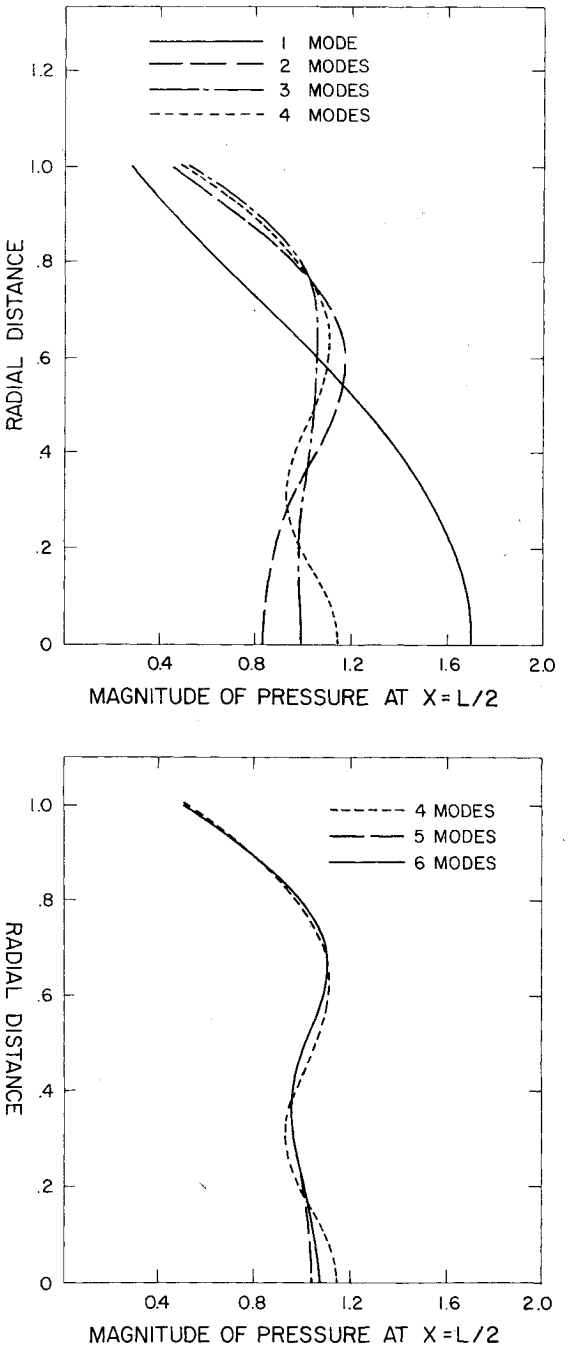

Fig. 3 Effect of increasing the number of modes on the convergence of the acoustic pressure profiles at the throat for a converging-diverging lined duct with no mean flow for $\omega=18$.

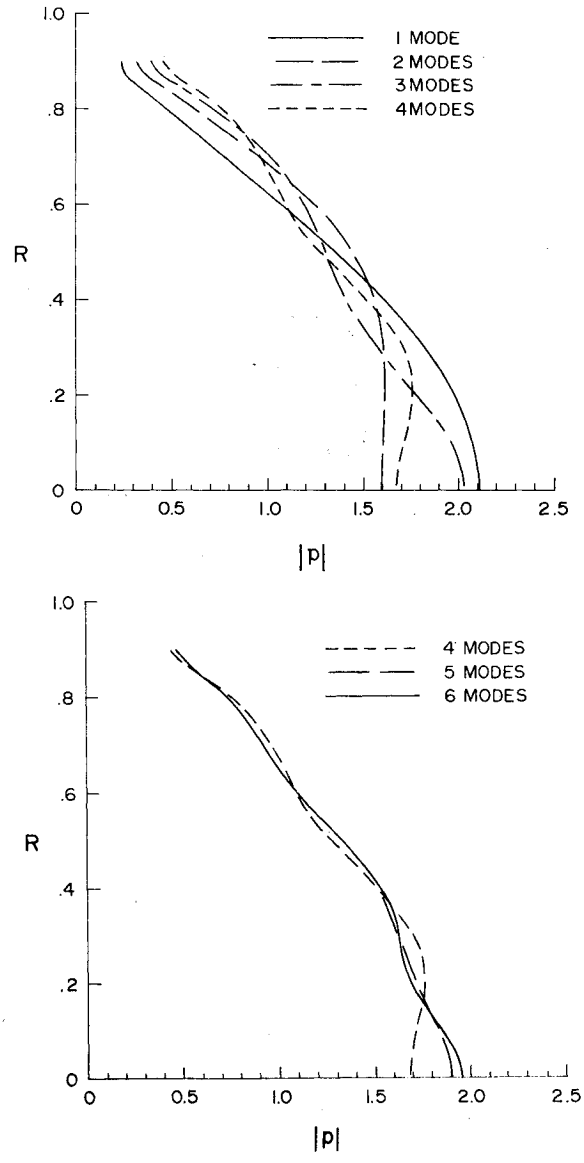

Fig. 4 Effect of increasing the number of modes on the convergence of the acoustic pressure profiles at the throat for a converging lined duct with flow; $\omega = 18$, $M_{throat} = -0.35$.

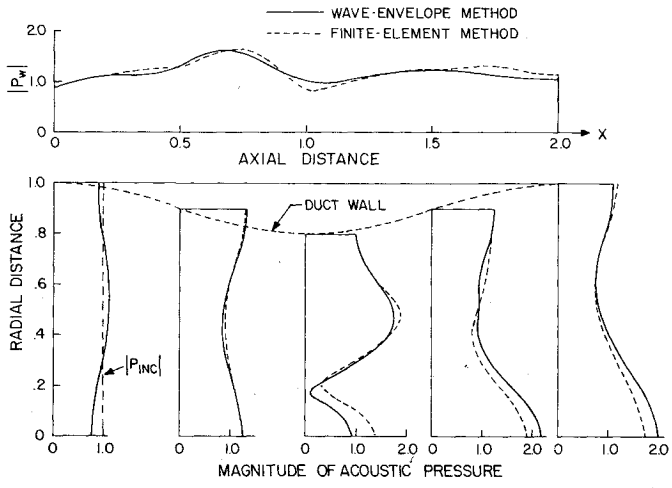

Fig. 5 Comparison of wave-envelope and finite-element methods for a converging-diverging hard-walled duct with no flow for $\omega = 9.12$.

and that changes are quite pronounced across the entire duct for the first four modes. Addition of the fifth and sixth modes produces small changes (this would not be true if the input signal contained significant amounts of these modes). In contrast, the transmission coefficients converge more rapidly as shown in Table 1. With four modes, the transmission coefficients of all the modes that can be calculated are accurate. The coefficient of the lowest mode is the slowest to converge. In the second example, a converging lined duct is considered; the mean Mach number varies from $M = -0.2$ at $x = 0$ to $M = -0.325$ at $x = 1$, and the boundary layer thickens as the mean flow expands from $x = 1$ to $x = 0$. Convergence of the acoustic pressure midway through the duct is illustrated in Fig. 4. The results are generally comparable to those obtained for no-mean flow, as are the results for convergence of the transmission and reflection coefficients.

Several cases have been set up for comparing the results of the wave-envelope procedure with the results from the finite-element procedure developed by Abrahamson.[24] The finite-element results have been supplied by H. Lester of Langley Research Center. The finite-element method was developed for a compressible mean flow, but is currently implemented with an incompressible model; hence, the cases chosen for comparison are for low-speed mean flows or for no-mean flow. The wave-envelope method specifies the mode amplitudes incident on the duct section at $x = 0$, specifies no input at $x = L$, and solves for the acoustic pressure distribution throughout the duct. The pressure distribution that results at $x = 0$ is used as input for the finite-element program, which specifies a $\rho_0 c_0$ impedance at $x = L$ to approximate the no-input boundary condition at that station. The pressure profiles from the two methods at $x/L = \frac{1}{4}, \frac{1}{2}, \frac{3}{4}$, and 1, as well as the axial variation of the pressure at the wall, are then computed.

The cases considered are for a dimensionless circular frequency of $\omega = 9.12$, at which there are three cut-on modes propagating in each direction. The comparison for no-mean flow is shown in Fig. 5. The incident signal at $x = 0$ is the fundamental plane mode and reflection in the duct results in the acoustic distribution shown in the left portion of the figure. Considerable variation of the acoustic profiles takes place as the signal propagates through the duct. The trends from the two methods of solution are the same, and the results agree reasonably well, except at the center of the duct near the throat. The variation of pressure along the outer wall is also quite pronounced, and both methods yield the same trends: the peak magnitude occurs ahead of the minimum area and a local minimum in pressure occurs close to the minimum area. Although the agreement is not exact, overall it is very satisfactory. The comparison for a case with a mean flow is similar with slightly larger differences between the methods.

For high Mach numbers, one-dimensional theories have been used in the literature; for example, Myers and Callegari[30] used such calculations to indicate the singular behavior of linear acoustic theory as the mean Mach number approaches unity. For their calculations, the duct area was described by a polynomial

$$R^2 = \frac{1}{2}\left[1 + 8\left(\frac{x}{L} - \frac{1}{2}\right)^2 - 16\left(\frac{x}{L} - \frac{1}{2}\right)^4\right]$$

and results were presented in the form of the ratio of the acoustic pressure amplitude to the incident pressure amplitude as a function of distance through the duct.

The wave-envelope method clearly is not a one-dimensional model; however, as many two-dimensional effects as possible have been suppressed to effect the closest possible agreement between conditions in the one-dimensional and wave-envelope calcualtions. Only one mode propagating in each direction is included, and the duct wall is taken to be rigid. The boundary-layer displacement thickness is set to a very small value

(0.001) in an attempt to minimize any refractive effects on the acoustic signal. In order to obtain the same axial variation of the mean flow in both calcualtions, the radius of the duct for the wave-envelope calculations has been taken to be

$$R=\left\{\frac{1}{2}\left[1+8\left(\frac{x}{L}-\frac{1}{2}\right)^2-16\left(\frac{x}{L}-\frac{1}{2}\right)^4\right]\right\}^{1/2}+\delta_1$$

and the displacement thickness is taken to be constant.

To suppress two-dimensional effects, we set the mean radial velocity equal to zero, take the wall temperature equal to the value at the centerline, and set the recovery fator to zero in order to eliminate any refractive effect from a transverse temperature gradient. Despite these restrictions, the wave-envelope method is still basically two-dimensional. For example, the acoustic particle velocity normal to the wall is required to be zero, whereas a one-dimensional model is equivalent to a zero acoustic velocity normal to the duct centerline. Hence, it is of interest to examine the differences between the results of the two approaches. In general, it has been found that the magnitude of the acoustic pressure is larger near the throat of the duct than is predicted by one-dimensional theory, especially when the throat Mach number is large. In addition, as the throat Mach number reaches high-subsonic values, a substantial refractive effect develops, even from the very small boundary layer that was used in this study. An example of these effects is shown in Fig. 6. The converging duct section results in a higher acoustic pressure in the throat region than is predicted by one-dimensional theory. The incident signal at $x=0$ propagates downstream, and an upstream wave is present as a consequence of reflections within the variable-area duct. In the throat region, the upstream wave has a very short wavelength; thus, the boundary layer produces a significant refraction of the upstream wave toward the duct centerline. The acoustic propagation in the throat region is not a one-dimensional process.

The effect of removing some of the "one-dimensional" restrictions has been examined. The results of Fig. 7 have been obtained with a constant wall temperature throughtout the duct, $T_w=1.0$; thus, the wall is hotter than the mean flow in the vicinity of the throat and a temperature-profile refractive effect occurs. This results in a further intensification of the acoustic pressure in the throat region. Finally, the influence of a mean radial velocity has been included and the results are shown in Fig. 8. The mean radial-velocity component has a strong effect on the acoustic pressure, reducing the pressure amplitude at the throat and bringing the two-dimensional results into closer agreement with one-dimensional theory than occurred in the two previous cases. In each of these cases, the input signal at $x=0$ is in the downstream direction, considerable reflection occurs as a result of the axial gradient, and hence there is a significant upstream propagating component at the throat of the converging-diverging duct section.

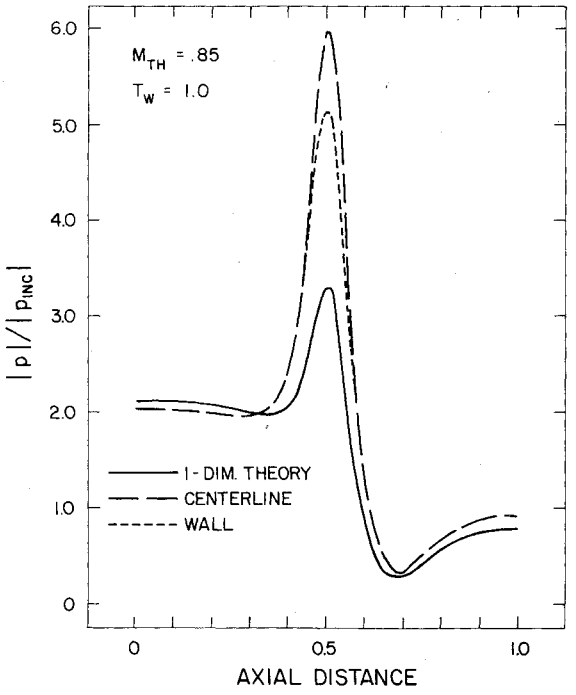

Fig. 7 Comparison of wave-envelope and one-dimensional theories for the case of a heated wall.

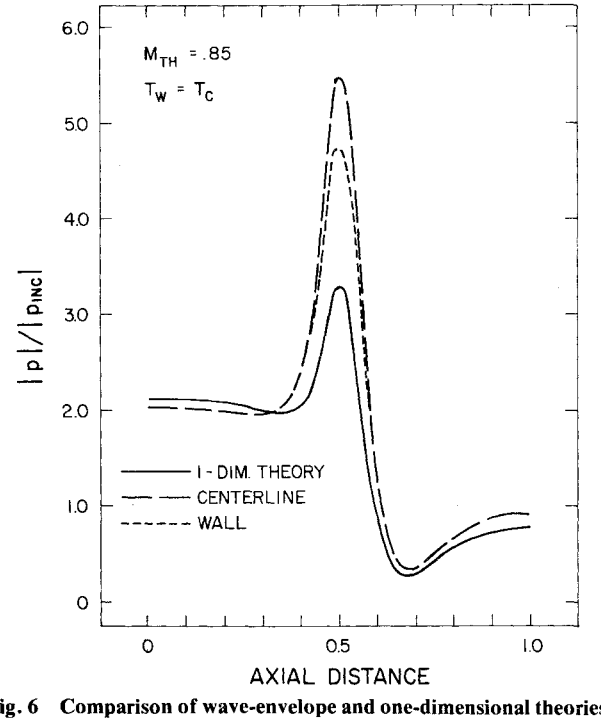

Fig. 6 Comparison of wave-envelope and one-dimensional theories.

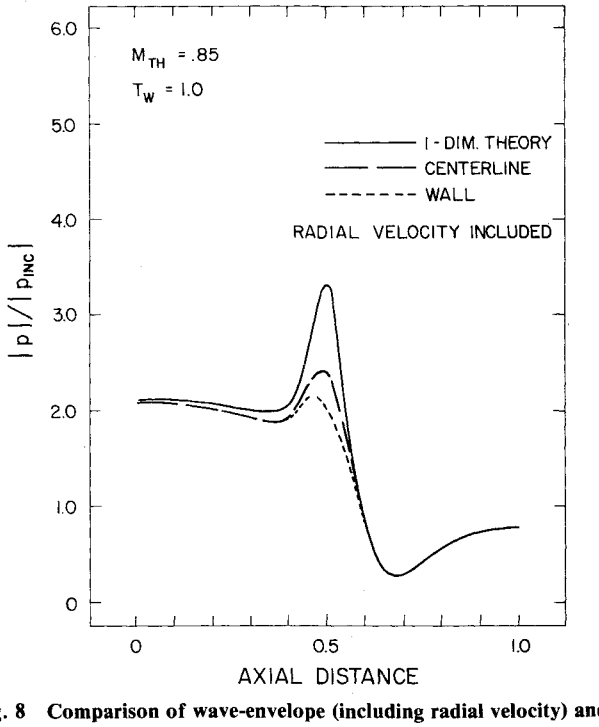

Fig. 8 Comparison of wave-envelope (including radial velocity) and one-dimensional theories.

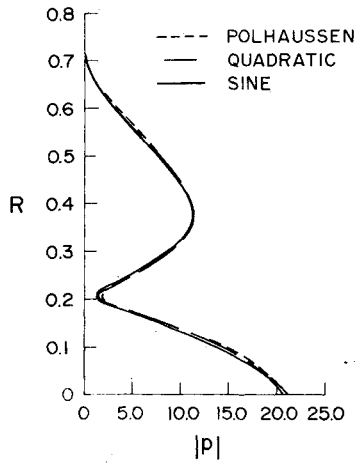

Fig. 9 Effect of boundary-layer velocity profile on the acoustic pressure profile in a converging hard-walled duct with flow, $\omega = 9$, $M_{throat} = -0.883$.

Currently underway is a detailed investigation of the intensification and refraction of acoustic signals in the high Mach number region of a simple converging duct section when the boundary-layer thickness is not artifically small as it was in the preceding examples. The influences of the Mach number, acoustic frequency, and duct-liner properties are being examined for both upstream and downstream input signals. These results will be presented at a later date. However, one simple result can be cited here. Despite the sensitivity of the acoustic results to changes in the mean-flow parameters, the refractive effects of the boundary layer are basically the same whether one uses a quarter-sine, quadratic, or Pohlhausen velocity profile, provided the boundary-layer displacement thickness is kept the same as shown in Fig. 9. This result is consistent with the conclusions reached in parallel-duct studies.[31]

VI. Summary

An acoustic theory is developed to determine the sound transmission and attenuation through an infinite, hard-walled or lined circular duct carrying compressible, sheared mean flows and having a variable cross section. The theory is applicable to large as well as small axial variations as long as the mean flow does not separate. The technique is based on solving for the envelopes of the quasiparallel acoustic modes that exist in the duct instead of solving for the actual wave, thereby reducing the computation time and the round-off error encountered in purely numerical techniques. The solution recovers the solution based on the method of multiple scales for slowly varying duct geometry.

A computer program has been developed based on the wave-envelope analysis for general mean flows. The mean-flow model consists of a one-dimensional flow in an inviscid core and a quarter-sine profile in the boundary layer. Mean radial velocity effects can be included. Numerical calculations performed for waves propagating in uniform ducts carrying fully developed mean flows agree with the well-known results for uniform ducts. For nonuniform ducts, results are presented for the reflection and transmission coefficients, as well as the acoustic pressure distributions for a number of conditions: both straight and variable-area ducts with and without liners and mean flows from very low- to high-subsonic speeds are considered. The results for transmission and reflection coefficients are shown to possess symmetry characteristics in those cases for which they are expected. Convergence of the transmission coefficients and of the acoustic pressure profiles with an increasing number of modes is illustrated. Comparisons with the results of a finite-element analysis for low-speed mean flows have shown reasonable agreement. Comparisons with one-dimensional results for high-speed mean flows have shown strong two-dimensional effects occurring near the duct throat.

Acknowledgment

This work was supported by the NASA Langley Research Center under Contrat No. NAS 1-13884.

References

[1] Greatrex, F. B., "By-Pass Engine Noise," *SAE Transactions*, Vol. 69, 1961, pp. 312-324.

[2] Sobel, J. A. and Welliver, A. D., "Sonic Block Silencing for Axial and Screw-Type Compressor," *Noise Control*, Vol. 7, No. 5, Sept./Oct. 1961, pp. 9-11.

[3] Nayfeh, A. H., Kaiser, J. E., and Telionis, D. P., "Acoustics of Aircraft Engine-Duct systems," *AIAA Journal*, Vol. 13, 1975, pp. 130-153.

[4] Nayfeh, A. H., "Sound Propagation Through Nonuniform Ducts," *Proceedings of the Society of Engineering Science at NASA-Langley Research Center*, Nov. 1976.

[5] Vaidya, P. G. and Dean, P. D., "State of the Art of Duct Acoustics," AIAA Paper 77-1279, 1977.

[6] Powell, A., "Theory of Sound Propagation Through Ducts Carrying High-Speed Flows," *Journal of the Acoustical Society of America*, Vol. 32, 1960, pp. 1640-1646.

[7] Eisenberg, N. A. and Kao, T. W., "Propagation of Sound Through a Variable-Area Duct with a Steady Compressible Flow," *Journal of the Acoustical Society of America*, Vol. 49, 1971, pp. 169-175.

[8] Davis, S. S. and Johnson, M. L., "Propagation of Plane Waves in a Variable Area Duct Carrying a Compressible Subsonic Flow," presented at the 87th Meeting of the Acoustical Society of America, New York, 1974.

[9] Huerre, P. and Karamcheti, K., "Propagation of Sound Through a Fluid Moving in a Duct of Varying Area," in *Interagency Symposium of University Research in Transportation Noise*, Stanford, Vol. II, 1973, pp. 397-413.

[10] King, L. S. and Karamecheti, L., "Propagation of Plane Waves in the Flow Through a Variable Area Duct," *Progress in Astronautics and Aeronautics: Aeroacoustics*, Vol. 31, edited by H. T. Nagamatsu, AIAA New York, 1975, pp. 403-418.

[11] Nayfeh, A. H., Telionis, D. P., and Lekoudis, S. G., "Acoustic Propagation in Ducts with Varying Cross Sections and Sheared Mean Flow," *Progress in Astronautics and Aeronautics: Aeroacoustics*, Vol. 37, edited by H. T. Nagamatsu, AIAA New York, 1975, pp. 331-351.

[12] Nayfeh, A. H., Kaiser, J. E., and Telionis, D. P., "Transmission of Sound Through Annular Ducts of Varying Cross Sections," *AIAA Journal*, Vol. 13, Jan. 1975, pp. 60-65.

[13] Nayfeh, A. H. and Kaiser, J. E., "Effect of Compressible Sheared Mean Flow on Sound Transmission Through Variable-Area Plane Ducts," AIAA Paper 75-128, 1975.

[14] Nayfeh, A. H., "Acoustic Waves in Ducts with Sinusoidally Perturbed Walls and Mean Flow," *Journal of the Acoustical Society of America*, Vol. 57, 1975, pp. 1036-1039.

[15] Quinn, D. W., "A Finite Difference Method for Computing Sound Propagation in Nonuniform Ducts," AIAA Paper 75-130, 1975.

[16] Baumeister, K. J. and Rice, E. J., "A Difference Theory for Noise Propagation in an Acoustically Lined Duct with Mean Flow," *Progress in Astronautics and Aeronautics: Aeroacoustics*, Vol. 37, edited by H. T. Nagamatsu, AIAA, New York, 1975, pp. 435-453.

[17] Baumeister, K. H., "Wave Envelope Analysis of Sound Propagation in Ducts with Variable Axial Impedance," *Progress in Astronautics and Aeronautics: Aeroacoustics*, Vol. 44, edited by I. R. Schwarz, AIAA, New York, 1976, pp. 451-474.

[18] Eversman, W., "A Multimodal Solution for the Transmission of Sound in Nonuniform Hard Wall Ducts with High Subsonic Flow," AIAA Paper 76-497, 1976.

[19] Zorumski, W. E., "Acoustic Theory of Axisymmetric Multisectioned Ducts," NASA TR R-419, May 1974.

[20] Kaiser, J. and Nayfeh, A. H., "A Wave-Envelope Technique for Wave Propagation in Nonuniform Ducts," *AIAA Journal*, Vol. 15, April 1977, pp. 533-537.

[21] Nayfeh, A. H., Shaker, B. S., and Kaiser, J. E., "Transmission of Sound Through Nonuniform Circular Ducts with Compressible Mean Flows," NASA CR-145126, Virginia Polytechnic Institute and State University, Blacksburg, Va., May 1977.

[22] Sigman, R. K., Majjigi, R. K., and Zinn, B. T., "Determination of Turbofan Inlet Acoustics Using Finite Elements," *AIAA Journal*, Vol. 16, 1978, pp. 1139-1145.

[23] Eversman, W., Astley, R. J., and Thanh, V. P., "Transmission in Nonuniform Ducts—A Comparative Evaluation of Finite Element

and Weighted Residuals Computation Schemes," AIAA Paper 77-1299, Oct. 1977.

[24] Abrahamson, A. L., "A Finite Element Model of Sound Propagation in a Nonuniform Circular Duct Containing Compressible Flow," AIAA Paper 77-1301, Oct. 1977.

[25] Schlichting, H., *Boundary-Layer Theory*, 6th ed., McGraw-Hill, New York, 1968.

[26] Nayfeh, A. H., *Perturbation Mthod*, Wiley-Interscience, New York, Chap. 6, 1973.

[27] Nayfeh, A. H., *Introduction to Perturbation Methods*, Wiley-Interscience, 1980, in press, Chap. 15.

[28] Hersh, A. S. and Catton, I., "Effects of Shear Flow on Sound Propagation in Rectangular Ducts," *The Journal of Acoustical Society of America*, Vol. 50, No. 3, Sept. 1971, pp. 992-1003.

[29] Unruh, J. F. and Eversman, W., "The Utility of the Galerkin Method for the Acoustic Transmission in an Attenuating Duct," *Journal of Sound and Vibration*, Vol. 23, No. 2, July 1972, pp. 187-197.

[30] Myers, M. K. and Callegari, A. J., "On the Singular Behavior of Linear Acoustic Theory in Near-Sonic Duct Flows," *Journal of Sound and Vibration*, Vol. 15, 1977, pp. 517-531.

[31] Nayfeh, A. H., Kaiser, J. E., and Shaker, B. S., "Effect of Mean-Velocity Profile Shapes on Sound Transmission Through Rectangular Ducts," *Journal of Sound and Vibration*, Vol. 34, No. 3, June 1974, pp. 413-423.